Multiuser Beam Tracking and Target Detection in Integrated Sensing and Communication

Kangjian Chen *†, Chenhao Qi *† and Octavia A. Dobre ‡
*School of Information Science and Engineering, Southeast University, Nanjing, China
†National Mobile Communications Research Laboratory, Southeast University, Nanjing, China
‡Faculty of Engineering and Applied Science, Memorial University, Canada
Email: {kjchen, qch}@seu.edu.cn, odobre@mun.ca

***Abstract*—In this paper, radar-aided multiuser beam tracking and target detection are investigated for integrated sensing and communication (ISAC). A multiuser beam tracking scheme based on the collaboration of radar sensing and uplink communication is proposed. It is first proved that the echoes of each communication signal can be extracted from the mixed echoes of multiple communication signals, by performing point-wise division and two-dimensional discrete Fourier transform. Based on it, the scheme enables the road side unit (RSU) to perform multiuser beam tracking and target detection with only two radio frequency chains, no matter how many users are served by the RSU. To distinguish the users from the targets and further improve the beam tracking by extended Kalman filtering, uplink pilots from the users to the RSU are employed. Then the digital beamformer can be designed to mitigate the multiuser interference. Simulation results show that the proposed scheme outperforms the conventional beam tracking scheme and can approach the performance of independent beam tracking of each user.**

***Index Terms*—Beam tracking, integrated sensing and communication (ISAC), multiuser interference, target detection.**

I. Introduction

Integrated sensing and communication (ISAC) has aroused wide attention due to its great potential in improving the overall performance of both the communication systems and the sensing systems [1]. Combining communication and sensing together enables the sharing of hardware and spectrum between the two originally independent systems, which not only saves the hardware costs and the installed space but also alleviates the rising shortage of spectrum resources. Besides, in the ISAC system, the communication or the sensing can operate with the seamless aid from the other functionality. As a result, both the performance of communication and the performance of sensing are enhanced [2].

Although ISAC has broad prospects in improving the spectrum efficiency, hardware efficiency and system performance, the development of ISAC faces numerous challenges, including the interference management, the resource allocation, the dual-functional designs, the efficient reciprocity, and so on. Many significant and interesting explorations have been conducted to overcome the difficulties [3]–[5]. In [3], the authors consider the coexistence of communication and sensing, where two reconfigurable intelligent surfaces are deployed for enhancing communication signals and suppressing mutual interference. In [4], the authors focus on the dual-functional beam design which aims at approaching the objective radar beam pattern under the communication performance constraints. In [5], the authors investigate the joint power allocation for the coexistence of radar and communication systems, where the radar and communication share the spectrum resources.

Particularly, ISAC is considered to be an important part in the vehicle to everything (V2X) networks because of the perfect match between the ISAC and the V2X. On one hand, the vehicles usually have large values of radar cross section (RCS) and high speed, which facilitates the radar sensing. On the other hand, the fast moving vehicles are more prone to the beam misalignment, which will deteriorate the performance of communication. Therefore, the researchers intend to exploit the sensing ability of road side unit (RSU) to assist the beam alignment of communication in the V2X networks [6]–[8]. In [6], the radar functionality of the RSU is exploited to sense the user and an extended Kalman filtering (EKF) framework is proposed to assist the communication beam tracking. In [7], a novel message passing algorithm based on factor graph is proposed to estimate the motion parameters of vehicles in real time. In [8], a radar-aided communication scheme, which focuses on extracting range and velocity information from the radar echoes, is proposed.

In this work, we propose a novel multiuser beam tracking scheme based on the collaboration of radar sensing and uplink communication. We first prove that the echoes of each communication signal can be extracted from the mixed echoes of multiple communication signal, by performing point-wise division and two-dimensional discrete Fourier transform. Based on it, the scheme enables the RSU to perform multiuser beam tracking and target detection with only two radio frequency chains, no matter how many users are served by the RSU. To distinguish the users from the targets and further improve the beam tracking by extended Kalman filtering, we employ uplink pilots from the users to the RSU. Then, we design the digital beamformer to mitigate the multiuser interference based on the uplink pilots.

The notations are defined as follows. $(\cdot)^{\mathrm{T}}$ and $(\cdot)^{\mathrm{H}}$ denote the transpose and conjugate transpose (Hermitian), respectively. $\mathbb{C}$, $\mathcal{N}$, $\mathcal{CN}$, $\mathbb{E}\{\cdot\}$, $\mathrm{Var}\{\cdot\}$, $\mathrm{Re}\{\cdot\}$, $\mathrm{Im}\{\cdot\}$, $\boldsymbol{I}_N$, j, $|\cdot|$

ICC 2023 - IEEE International Conference on Communications | 978-1-5386-7462-8/23/$31.00 ©2023 IEEE | DOI: 10.1109/ICC45041.2023.10279142

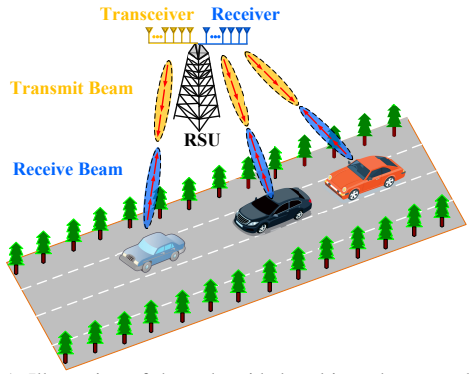

Fig. 1: Illustration of the radar-aided multiuser beam tracking.

and $\|\cdot\|_2$ denote the set of complex number, the Gaussian distribution, the complex Gaussian distribution, the expectation of a random variable, the variance of a random variable, the real part of a complex number, the imaginary part of a complex number, an $N \times N$ identity matrix, the square root of -1, the absolute value of a scalar and ℓ_2-norm of a vector, respectively.

II. System Model

As shown in Fig. 1, we consider the radar-aided multiuser beam tracking for the RSU, where a MIMO-OFDM RSU consisting of a communication transceiver and a collocated receiver serves K moving users. The hybrid beamforming structure is adopted at both the transceiver and the receiver while the analog beamforming structure is adopted at each user to improve the energy efficiency. The transceiver is equipped with M_{T} radio frequency (RF) chains and an N_{T}-antenna uniform linear array (ULA). The receiver is equipped with M_{R} RF chains and an N_{R}-antenna ULA. For each user, an N_{U}-antenna ULA is employed. The antenna spacing of all the antenna arrays is $d = \lambda_{\mathrm{c}}/2$, where λ_{c} is the wavelength of the carrier frequency. The number of subcarriers is denoted as S. Suppose the block-wise OFDM transmission is adopted, where the number of symbols in a block is denoted as P. The beamformers at both the transceiver and the receiver are assumed to be the same in one block. During the communication, the transceiver sends data streams to the users. Meanwhile, the receiver collects the echoes from the T targets, which consists of K users and $T-K$ non-cooperative targets. Then, for the pth symbol on the sth subcarrier, the received signals at the receiver of the RSU can be expressed as

$$\boldsymbol{y}_s^{(p)} = \boldsymbol{W}_{\mathrm{RF}}^{\mathrm{H}} \boldsymbol{H}_{\mathrm{r},s}^{(p)} \boldsymbol{F}_{\mathrm{RF}} \widetilde{\boldsymbol{x}}_s^{(p)} + \boldsymbol{W}_{\mathrm{RF}}^{\mathrm{H}} \boldsymbol{\eta}_{\mathrm{r}}, \tag{1}$$

where $\boldsymbol{W}_{\mathrm{RF}} \in \mathbb{C}^{N_{\mathrm{R}} \times M_{\mathrm{R}}}$ denotes the analog beamformer at the receiver, $\boldsymbol{F}_{\mathrm{RF}} \in \mathbb{C}^{N_{\mathrm{T}} \times M_{\mathrm{T}}}$ denotes the analog beamformer at the transceiver, $\widetilde{\boldsymbol{x}}_s^{(p)} \triangleq \boldsymbol{F}_{\mathrm{BB},s} \boldsymbol{x}_s^{(p)}$, $\boldsymbol{F}_{\mathrm{BB},s} \in \mathbb{C}^{M_{\mathrm{T}} \times K}$ denotes the digital beamformer, $\boldsymbol{x}_s^{(p)} \in \mathbb{C}^{K \times 1}$ denotes the modulated symbols and $\boldsymbol{\eta}_{\mathrm{r}} \sim \mathcal{CN}(0, \sigma_{\mathrm{r}}^2 \boldsymbol{I}_{N_{\mathrm{R}}})$ denotes the additive white Gaussain noise (AWGN). In (1), the digital beamformer at the receiver is set as the identity matrix, which implies that we only need the analog beamformer to perform the proposed multiuser beam tracking scheme. $\boldsymbol{H}_{\mathrm{r},s}^{(p)}$ denotes the reflected channel of the T targets, which can be expressed as

$$\boldsymbol{H}_{\mathrm{r},s}^{(p)} = \sum_{i=1}^{T} \gamma_{s,p}^{(i)} \boldsymbol{\alpha}\left(N_{\mathrm{R}}, \theta_{\mathrm{r}}^{(i)}\right) \boldsymbol{\alpha}\left(N_{\mathrm{T}}, \theta_{\mathrm{r}}^{(i)}\right)^{\mathrm{H}}, \tag{2}$$

where $\gamma_{s,p}^{(i)} \triangleq g_{\mathrm{r}}^{(i)} e^{-j2\pi(s-1)\tau_{\mathrm{r}}^{(i)}\Delta f} e^{j2\pi(p-1)f_{\mathrm{r}}^{(i)}T_{\mathrm{s}}}$, $g_{\mathrm{r}}^{(i)}$, $\tau_{\mathrm{r}}^{(i)}$, $f_{\mathrm{r}}^{(i)}$ and $\theta_{\mathrm{r}}^{(i)}$ denote the channel gain, the channel delay, the Doppler frequency and the channel angle-of-departure (AoD) of the ith target, respectively. Δf and T_{s} denote the subcarrier spacing and the duration of one OFDM symbol. The function $\boldsymbol{\alpha}(\cdot)$ denotes the channel steering vector and can be expressed as

$$\boldsymbol{\alpha}(N, \theta) = [1, e^{j\theta}, \cdots, e^{j(N-1)\theta}]^{\mathrm{T}}. \tag{3}$$

To support high-speed transmission, a large-scale antenna array is equipped at the RSU to form directional beams, which increases the training overhead for beam alignment while providing high beam gains [9], [10]. An efficient way to reduce the overhead for beam alignment is the beam tracking [6]. Based on the assumption that the echoes from the user and the downlink communication to the user experience the same channel, the beam tracking problem based on communication pilots is equivalently converted to the target tracking problem based on sensing [6]–[8]. Then, the angles of users extracted from the echoes in (1) are used to assist the beam alignment for communication.

Although the procedure above works well for the single-user scenario, some critical issues for the multiuser scenarios are missed:

1) Different from the sensing procedure in conventional radar systems that transmit unified waveform for all targets, the RSU simultaneously transmits multiple data streams with multi-directional beams to users. As a result, the received signals in (1) contain echoes of multiple data streams. Novel sensing schemes for multiuser scenarios are needed.

2) In practice, both cooperative users and non-cooperative targets exist in the coverage of the RSU, where motion parameters of the cooperative users are what the RSU is interested in. The conventional radar sensing distinguishes the users from non-cooperative targets based on the kinematic model, which is error-prone especially when the users and targets are crowded. What is worse, the conventional radar sensing can not correctly distinguish the users from targets if the confusion between the users and the targets happens. How to identify each user from other users or targets needs to be considered.

3) As shown in Fig. 1, the RSU serves multiple users simultaneously, where multiuser interference exists in the system inevitably due to the multipath effects and the energy leakage. However, the existing procedure transmits data streams only relying on the estimated line-of-sight (LoS) paths, which misses the important part of multiuser interference cancellation. How to effectively eliminate the multiuser interference needs to be considered.

In this work, to solve the three issues above, we propose a radar-aided multiuser beam tracking based on the collabora-

tion of communication and sensing, which will be discussed in the next section.

III. Radar-aided Multiuser Beam Tracking

In this section, we first extract the echoes of each communication signal from the mixed echoes of multiple communication signals by performing point-wise division and two-dimensional discrete Fourier transform. Then, we perform target detection based on the extracted echoes with only two radio frequency chains. To distinguish the users from the targets and further improve the beam tracking by extended Kalman filtering, we employ uplink pilots from the users to the RSU taking the cooperativeness of the users into account. After that, we design the digital beamformer to mitigate the multiuser interference based on the uplink pilots.

A. Extraction of Echoes for Each User

To perform the multiuser beam tracking, we first focus on the echoes of the T targets in (1) to obtain $\theta_{\mathrm{r}}^{(i)}$, $\tau_{\mathrm{r}}^{(i)}$ and $f_{\mathrm{r}}^{(i)}$ based on the received signal $\boldsymbol{y}_s^{(p)}$. Note that the transceiver and the receiver of the RSU are collocated. Therefore, it is convenient for the receiver to get the duplication of the transmit signals. Then, by performing the point-wise division, we can obtain

$$\begin{aligned}\boldsymbol{z}_{k,s}^{(p)} &= \boldsymbol{y}_s^{(p)}/[\widetilde{\boldsymbol{x}}_s^{(p)}]_k \\ &= \sum_{m=1,m\neq k}^{K} \boldsymbol{W}_{\mathrm{RF}}^{\mathrm{H}} \boldsymbol{H}_{\mathrm{r},s}^{(p)} [\boldsymbol{F}_{\mathrm{RF}}]_{:,m} \frac{[\widetilde{\boldsymbol{x}}_s^{(p)}]_m}{[\widetilde{\boldsymbol{x}}_s^{(p)}]_k} \\ &\quad + \boldsymbol{W}_{\mathrm{RF}}^{\mathrm{H}} \boldsymbol{H}_{\mathrm{r},s}^{(p)} [\boldsymbol{F}_{\mathrm{RF}}]_{:,k} + \widetilde{\boldsymbol{\eta}}_{\mathrm{r}}, \end{aligned} \tag{4}$$

where $\widetilde{\boldsymbol{\eta}}_{\mathrm{r}} \triangleq \boldsymbol{W}_{\mathrm{RF}}^{\mathrm{H}} \boldsymbol{\eta}_{\mathrm{r}}/[\widetilde{\boldsymbol{x}}_s^{(p)}]_k$. We take the received signals of the bth RF chain as an example and stack the bth entry of $\boldsymbol{z}_{k,s}^{(p)}$ for the S subcarriers and the P symbols as $\boldsymbol{Z}_k^{(b)} \in \mathbb{C}^{S\times P}$. Denote the $N\times N$ DFT matrix for arbitrary N as $\boldsymbol{D}_N$. Then, we have

$$\begin{aligned}\widehat{\boldsymbol{Z}}_k^{(b)} &= \boldsymbol{D}_S^{\mathrm{H}} \boldsymbol{Z}_k^{(b)} \boldsymbol{D}_P \\ &= \sum_{m=1,m\neq k}^{K} \sum_{i=1}^{T} G_m^{(i)} \boldsymbol{D}_S^{\mathrm{H}} (\boldsymbol{\Lambda}^{(i)} \circ \boldsymbol{X}_m) \boldsymbol{D}_P \\ &\quad + \sum_{i=1}^{T} G_k^{(i)} \boldsymbol{D}_S^{\mathrm{H}} \boldsymbol{\Lambda}^{(i)} \boldsymbol{D}_P + \boldsymbol{N}, \end{aligned} \tag{5}$$

where

$$\begin{aligned} &G_m^{(i)} = g_{\mathrm{r}}^{(i)} \boldsymbol{w}_b^{\mathrm{H}} \boldsymbol{\alpha}\left(N_{\mathrm{R}}, \theta_{\mathrm{r}}^{(i)}\right) \boldsymbol{\alpha}\left(N_{\mathrm{T}}, \theta_{\mathrm{r}}^{(i)}\right)^{\mathrm{H}} \boldsymbol{f}_m, \\ &G_k^{(i)} = g_{\mathrm{r}}^{(i)} \boldsymbol{w}_b^{\mathrm{H}} \boldsymbol{\alpha}\left(N_{\mathrm{R}}, \theta_{\mathrm{r}}^{(i)}\right) \boldsymbol{\alpha}\left(N_{\mathrm{T}}, \theta_{\mathrm{r}}^{(i)}\right)^{\mathrm{H}} \boldsymbol{f}_k, \\ &\boldsymbol{w}_b = [\boldsymbol{W}_{\mathrm{RF}}]_{:,b},\ \boldsymbol{f}_m = [\boldsymbol{F}_{\mathrm{RF}}]_{:,m},\ \boldsymbol{f}_k = [\boldsymbol{F}_{\mathrm{RF}}]_{:,k}, \\ &[\boldsymbol{\Lambda}^{(i)}]_{s,p} = e^{-j2\pi(s-1)\tau_{\mathrm{r}}^{(i)}\Delta f} e^{j2\pi(p-1)f_{\mathrm{r}}^{(i)}T_{\mathrm{s}}}, \\ &[\boldsymbol{X}_m]_{s,p} = [\widetilde{\boldsymbol{x}}_s^{(p)}]_m/[\widetilde{\boldsymbol{x}}_s^{(p)}]_k. \end{aligned} \tag{6}$$

and $\boldsymbol{N}$ is the AWGN matrix regarding the fact that the linear combination of independent Gaussian random variables is still a Gaussian random variable. In (5), $\widehat{\boldsymbol{Z}}_k^{(b)}$ consists of $\boldsymbol{D}_S^{\mathrm{H}} \boldsymbol{\Lambda}^{(i)} \boldsymbol{D}_P$ and $\boldsymbol{D}_S^{\mathrm{H}} (\boldsymbol{\Lambda}^{(i)} \circ \boldsymbol{X}_m) \boldsymbol{D}_P$, where the former denotes the reflections of the kth data stream and the latter denotes the reflections of other data streams. To unveil the properties of $\boldsymbol{D}_S^{\mathrm{H}} (\boldsymbol{\Lambda}^{(i)} \circ \boldsymbol{X}_m) \boldsymbol{D}_P$, we have the follow Lemma.

Lemma 1. *Define $\boldsymbol{A} \triangleq \boldsymbol{D}_S^{\mathrm{H}} (\boldsymbol{\Lambda}^{(i)} \circ \boldsymbol{X}_m) \boldsymbol{D}_P$. When PS tends to infinity, each entry of $\boldsymbol{A}$ converges to the Gaussian distribution.*

proof: see Appendix A.

Lemma 1 indicates that when detecting the kth user, we can focus on the echoes of the communication signal for the kth user and treat the echoes of other communication signals as the Gaussian noise if PS is large. In other words, the echoes of the communication signal for the kth user can be separated from the mixed echoes of the multiple communication signals with the point-wise division in (4) and the two-dimensional Fourier transform in (5), which enables the RSU to collect the echoes of multiple users for target detection with only one RF chain.

B. Target Sensing

According to **Lemma 1**, the received signals for the kth user in (5) can be rewritten as

$$\begin{aligned}\overline{\boldsymbol{Z}}_k^{(b)} &= \sum_{i=1}^{T} G_k^{(i)} \boldsymbol{D}_S^{\mathrm{H}} \boldsymbol{\Lambda}^{(i)} \boldsymbol{D}_P + \widetilde{\boldsymbol{N}} \\ &= \sum_{i=1}^{T} G_k^{(i)} \sqrt{PS} \boldsymbol{c}\boldsymbol{d}^{\mathrm{T}} + \widetilde{\boldsymbol{N}}, \end{aligned} \tag{7}$$

where

$$\begin{aligned} &\widetilde{\boldsymbol{N}} = \sum_{m=1,m\neq k}^{K} \sum_{i=1}^{T} G_m^{(i)} \boldsymbol{D}_S^{\mathrm{H}} (\boldsymbol{\Lambda}^{(i)} \circ \boldsymbol{X}_m) \boldsymbol{D}_P + \boldsymbol{N}, \\ &[\boldsymbol{c}]_s = \Xi(S, 2(s-1)/S - 2\tau_{\mathrm{r}}^{(i)}\Delta f), \\ &[\boldsymbol{d}]_p = \Xi(P, 2f_{\mathrm{r}}^{(i)}T_{\mathrm{s}} - 2(p-1)/P), \\ &\Xi(N,\psi) = e^{j(N-1)\pi/2} \sin(N\psi\pi/2)/\sin(\psi\pi/2). \end{aligned} \tag{8}$$

Note that $\overline{\boldsymbol{Z}}_k^{(b)}$ in (7) denotes the well-known range-velocity map, which contains the range and velocity information of targets [11]. To improve the detection performance of the targets from the range-velocity map, the analog beamformer $\boldsymbol{F}_{\mathrm{RF}}$ and the analog beamformer $\boldsymbol{w}_b$ need to be designed to form directional beams. Recall that the block-wise OFDM transmission is adopted in (1). Based on the assumption that the angles of users are approximately invariant for a block, we can perform beam tracking block by block. Suppose the predicted AoD for the kth user at the tth block for $t \geq 2$ is denoted as $\overline{\theta}_k^{(t)}$, where the case when $t = 1$ can be obtained with the existing channel estimation methods, such as [12]. We design $\boldsymbol{F}_{\mathrm{RF}}$ for the tth block as

$$\left[\overline{\boldsymbol{F}}_{\mathrm{RF}}^{(t)}\right]_{:,k} = \sqrt{N_{\mathrm{T}}} \boldsymbol{\alpha}\left(N_{\mathrm{T}}, \overline{\theta}_k^{(t)}\right). \tag{9}$$

We then turn to the design of the analog beamformer $\boldsymbol{w}_b$ at the receiver. Two objectives need to be achieved via the design of $\boldsymbol{w}_b$. The first objective is to form directional beams

to receive the echoes of the K users and the second objective is to obtain the angles of the targets by designing $\boldsymbol{w}_b$ for $b = 1, 2, \cdots, M_{\mathrm{R}}$. As the analog beamformer is used to receive echoes of the K users, it is natural to assume that $\boldsymbol{w}_b$ has equal beam gains along the K directions. Then, we formulate the design of $\boldsymbol{w}_b$ as

$$\begin{aligned} &\max_{\boldsymbol{w}_b} \min_{k=1,2,\cdots,K} \left| \boldsymbol{w}_b^{\mathrm{H}} \boldsymbol{\alpha}\left(N_{\mathrm{R}}, \overline{\theta}_k^{(t)}\right)\right| \\ &\text{s.t.} \quad |[\boldsymbol{w}_b]_m| = 1/\sqrt{N_{\mathrm{R}}},\ m = 1, 2, \cdots, N_{\mathrm{R}}. \end{aligned} \tag{10}$$

We solve (10) following the method in [13] and denote the solution as $\overline{\boldsymbol{w}}_b^{(t)}$. Then, we focus on the second objective. To determine the LoS path of one target, two independent receptions with two RF chains are needed, i.e., $M_{\mathrm{R}} = 2$. Borrowing the idea from the [14], the analog beamformers for the two RF chains are designed as

$$\widetilde{\boldsymbol{w}}_1 = [\widehat{\boldsymbol{w}}, 0]^{\mathrm{T}},\ \widetilde{\boldsymbol{w}}_2 = [0, \widehat{\boldsymbol{w}}]^{\mathrm{T}},\ \widehat{\boldsymbol{w}} = \left[\overline{\boldsymbol{w}}_b^{(t)\mathrm{T}}\right]_{1:N_{\mathrm{R}}-1}. \tag{11}$$

Substituting $\boldsymbol{w}_b = \widetilde{\boldsymbol{w}}_1$ and $\boldsymbol{w}_b = \widetilde{\boldsymbol{w}}_2$ to (7) in turn, we denote the received signals for the kth data stream as $\widetilde{\boldsymbol{Z}}_k^{(1)}$ and $\widetilde{\boldsymbol{Z}}_k^{(2)}$, respectively. As $\widetilde{\boldsymbol{Z}}_k^{(1)}$ and $\widetilde{\boldsymbol{Z}}_k^{(2)}$ have similar structure, we detect the targets from $\widetilde{\boldsymbol{Z}}_k^{(1)}$ without loss of generality. A widely adopted way to detect targets from the range-velocity map $\widetilde{\boldsymbol{Z}}_k^{(1)}$ is the constant false alarm rate (CFAR) detector [11]. As the CFAR detector is mature, we omit the detailed procedure and denote the set of the indices of the detection results as $\boldsymbol{\Psi} = \{(\widehat{s}_1, \widehat{p}_1), (\widehat{s}_2, \widehat{p}_2), \cdots, (\widehat{s}_Q, \widehat{p}_Q)\}$, where Q denotes the number of detected targets, $\widehat{s}_q$ and $\widehat{p}_q$ for $q = 1, 2, \cdots, Q$ denote the row index and the column index of the qth detected target on the range-velocity map, respectively. The estimated range and the estimated velocity of the qth detected target can be expressed as

$$\widehat{r}_q = \frac{(\widehat{s}_q - 1)c}{S\Delta f}, \qquad \widehat{v}_q = \frac{(\widehat{p}_q - 1)\lambda_{\mathrm{c}}}{PT_{\mathrm{s}}}, \tag{12}$$

where c denotes the speed of light. For the qth target, we focus on the entry on the $\widehat{s}_q$th row and the $\widehat{p}_q$th column of $\widetilde{\boldsymbol{Z}}_k^{(1)}$ and $\widetilde{\boldsymbol{Z}}_k^{(2)}$, which have the largest power. Then, we have

$$\Gamma_q = \left[\widetilde{\boldsymbol{Z}}_k^{(2)}\right]_{\widehat{s}_q, \widehat{p}_q} / \left[\widetilde{\boldsymbol{Z}}_k^{(1)}\right]_{\widehat{s}_q, \widehat{p}_q} \approx e^{j\pi\vartheta_q}, \tag{13}$$

where ϑ_q denotes the angle of the qth detected target. The estimation of ϑ_q is denoted as

$$\widehat{\vartheta}_q = \mathrm{ang}\left\{\Gamma_q\right\}/\pi, \tag{14}$$

where $\mathrm{ang}(\cdot)$ denotes the phase of a complex number.

C. Collaboration of Communication and Sensing

In Sec. III-B, Q targets are detected within the communication beam coverage of $\left[\overline{\boldsymbol{F}}_{\mathrm{RF}}^{(t)}\right]_{:,k}$. To identify the kth user from the Q targets, we intend to employ a small number of uplink pilots from the users to the RSU.

Suppose the beam alignment at the user has been completed and the designed analog beamformer of the kth user is denoted as $\widehat{\boldsymbol{v}}_k$. Then, the kth user transmits N_{P} uplink pilots to the RSU with $\widehat{\boldsymbol{v}}_k$. The nth received signal for the kth user at the RSU is expressed as

$$u_{k,s}^{(n)} = \widetilde{\boldsymbol{f}}_k^{(n)\mathrm{H}} \boldsymbol{H}_{k,s}^{(n)} \widehat{\boldsymbol{v}}_k + \widetilde{\boldsymbol{f}}_k^{(n)\mathrm{H}} \boldsymbol{\eta}_{\mathrm{c}}, \tag{15}$$

where $\widetilde{\boldsymbol{f}}_k^{(n)}$ denotes the hybrid beamformer for the kth user and $\boldsymbol{\eta}_{\mathrm{c}} \sim \mathcal{CN}(0, \sigma_{\mathrm{c}}^2 \boldsymbol{I}_{N_{\mathrm{U}}})$ denotes the AWGN. In (15), we set the transmit symbols as "1". $\boldsymbol{H}_{k,s}^{(n)}$ denotes the channel between the transceiver and the kth user, which can be expressed as

$$\boldsymbol{H}_{k,s} = \sum_{l=1}^{L_k} \chi_{s,p}^{(l)} \boldsymbol{\alpha}\left(N_{\mathrm{T}}, \phi_k^{(l)}\right) \boldsymbol{\alpha}\left(N_{\mathrm{U}}, \psi_k^{(l)}\right)^{\mathrm{H}}, \tag{16}$$

where $\chi_{s,p}^{(l)} \triangleq \widetilde{g}_k^{(l)} e^{-j2\pi(s-1)\tau_k^{(l)}\Delta f} e^{j2\pi(p-1)f_k^{(l)}T_{\mathrm{s}}}$, L_k, $\widetilde{g}_k^{(l)}$, $\tau_k^{(l)}$, $f_k^{(l)}$, $\phi_k^{(l)}$ and $\psi_k^{(l)}$ denote the number of paths, the channel gain, the propagation delay, the Doppler effect, the channel angle-of-arrival (AoA) and the channel AoD of the lth path between the kth user and the transmitter, respectively. Similar to (11), we set $N_{\mathrm{P}} = 2$, and design $\widetilde{\boldsymbol{f}}_k^{(n)}$ as

$$\widetilde{\boldsymbol{f}}_k^{(1)} = [\widehat{\boldsymbol{f}}, 0]^{\mathrm{T}}, \widetilde{\boldsymbol{f}}_k^{(2)} = [0, \widehat{\boldsymbol{f}}]^{\mathrm{T}}, \widehat{\boldsymbol{f}} = [[\overline{\boldsymbol{F}}_{\mathrm{RF}}^{(t)}]_{:,k}]_{1:N_{\mathrm{T}}-1}^{\mathrm{T}}. \tag{17}$$

Stack the received signals for the kth user as $\boldsymbol{U}_k \triangleq [\boldsymbol{u}_1, \boldsymbol{u}_2]$, where $\boldsymbol{u}_n = [u_{k,1}^{(n)}, u_{k,2}^{(n)}, \cdots u_{k,S}^{(n)}]$ for $n \in \{1, 2\}^{\mathrm{T}}$. We identify the kth user from the Q detected targets through a least square approach, which can be expressed as

$$q^* = \arg \min_{q=1,2,\cdots,Q} \left\| \boldsymbol{U}_k - \frac{\mathrm{tr}(\widetilde{\boldsymbol{U}}_q^{\mathrm{H}} \boldsymbol{U}_k)}{\mathrm{tr}(\widetilde{\boldsymbol{U}}_q^{\mathrm{H}} \widetilde{\boldsymbol{U}}_q)} \widetilde{\boldsymbol{U}}_q \right\|_F, \tag{18}$$

where

$$[\widetilde{\boldsymbol{U}}_q]_{s,n} = e^{-j2\pi(s-1)\Delta f \frac{\widehat{r}_q}{c}} e^{j2\pi(n-1)T_{\mathrm{s}} \frac{\widehat{v}_q}{\lambda_{\mathrm{c}}}} \widetilde{\boldsymbol{f}}_k^{(n)\mathrm{H}} \boldsymbol{\alpha}\left(N_{\mathrm{T}}, \widehat{\theta}_q\right).$$

We solve (18) by testing all the Q detected targets one by one. The estimated parameters of the kth user are denoted as

$$\widetilde{r}_k^t = \widehat{r}_{q^*},\ \ \widetilde{v}_k^t = \widehat{v}_{q^*}\ \ \widetilde{\theta}_k^t = \widehat{\vartheta}_{q^*}. \tag{19}$$

Define the kinematic parameters of the kth user at the tth block as $\boldsymbol{s}_k[t] = [x[t], y[t], v_x[t], v_y[t]]^{\mathrm{T}}$, where $x[t]$, $y[t]$, $v_x[t]$ and $v_y[t]$ denote the x-axis coordinate, the y-axis coordinate, the velocity component in the x-axis direction and the velocity component in the y-axis direction. Then, the estimated parameters of the kth user in (19) and the predicted state vector $\overline{\boldsymbol{s}}_k[t]$ are exploited by the widely-adopted EKF for target tracking. The filtered state vector at tth block after performing EKF is denoted as $\widetilde{\boldsymbol{s}}_k[t]$. Then, the predicted state vector for $(t+1)$th block is expressed as

$$\overline{\boldsymbol{s}}_k[t+1] = \begin{bmatrix} 1 & 0 & \Delta T & 0 \\ 0 & 1 & 0 & \Delta T \\ 0 & 0 & 1 & 0 \\ 0 & 0 & 0 & 1 \end{bmatrix} \widetilde{\boldsymbol{s}}_k[t], \tag{20}$$

where ΔT denotes the duration of one block. The predicted angle of the kth user is computed as

$$\overline{\theta}_k^{t+1} = \arctan(y[t+1]/x[t+1]). \tag{21}$$

Then $\overline{\boldsymbol{F}}_{\mathrm{RF}}^{t+1}$ can be designed via (9) and the beam tracking at the RSU is completed.

Algorithm 1 Radar-aided Multiuser Beam Tracking Scheme

1: **Input:** N_{T}, N_{R}, M_{T}, M_{R}, S, P, Δf, T_{s}, K, ΔT, $\overline{\theta}_k^t$.
2: Obtain $\widetilde{\boldsymbol{Z}}_k^{(1)}$ and $\widetilde{\boldsymbol{Z}}_k^{(2)}$ via (7).
3: Obtain $\widehat{r}_q$, $\widehat{v}_q$ and $\widehat{\vartheta}_q$ via (12) and (14).
4: Obtain $\widetilde{r}_k^t$, $\widetilde{v}_k^t$, and $\widetilde{\theta}_k^t$ via (19). Obtain $\overline{\theta}_k^{t+1}$ via (21).
5: Obtain $\overline{\boldsymbol{F}}_{\mathrm{RF}}^{t+1}$ via (9). Obtain $\overline{\boldsymbol{F}}_{\mathrm{BB},s}^{t+1}$ via (23).
6: **Output:** $\overline{\boldsymbol{F}}_{\mathrm{RF}}^{t+1}$ and $\overline{\boldsymbol{F}}_{\mathrm{BB},s}^{t+1}$.

D. Multiuser Interference Mitigation

After obtaining $\overline{\boldsymbol{F}}_{\mathrm{RF}}^{t+1}$, the K users transmit uplink pilots to mitigate the multiuser interference. Stacking $\{u_{k,s}, k = 1, 2, \cdots, K\}$ in (4) together as $\overline{\boldsymbol{u}}_s = [u_{1,s}, u_{2,s}, \cdots, u_{K,s}]^{\mathrm{T}}$, where the superscript "(n)" is omitted because only one pilot for each user is needed. Define $\overline{\boldsymbol{f}}_k \triangleq [\overline{\boldsymbol{F}}_{\mathrm{RF}}^{t+1}]_{:,k}$ we have $\overline{\boldsymbol{u}}_s = \boldsymbol{F}_{\mathrm{BB},s}^{\mathrm{H}} \boldsymbol{H}_{\mathrm{e},s}$, where

$$\boldsymbol{H}_{\mathrm{e},s} = \begin{bmatrix} \overline{\boldsymbol{f}}_1^{\mathrm{H}} \boldsymbol{H}_{1,s} \widehat{\boldsymbol{v}}_1 & \overline{\boldsymbol{f}}_1^{\mathrm{H}} \boldsymbol{H}_{2,s} \widehat{\boldsymbol{v}}_2 & \cdots & \overline{\boldsymbol{f}}_1^{\mathrm{H}} \boldsymbol{H}_{K,s} \widehat{\boldsymbol{v}}_K \\ \overline{\boldsymbol{f}}_2^{\mathrm{H}} \boldsymbol{H}_{1,s} \widehat{\boldsymbol{v}}_1 & \overline{\boldsymbol{f}}_2^{\mathrm{H}} \boldsymbol{H}_{2,s} \widehat{\boldsymbol{v}}_2 & \cdots & \overline{\boldsymbol{f}}_2^{\mathrm{H}} \boldsymbol{H}_{K,s} \widehat{\boldsymbol{v}}_K \\ \vdots & \vdots & \ddots & \vdots \\ \overline{\boldsymbol{f}}_K^{\mathrm{H}} \boldsymbol{H}_{1,s} \widehat{\boldsymbol{v}}_1 & \overline{\boldsymbol{f}}_K^{\mathrm{H}} \boldsymbol{H}_{2,s} \widehat{\boldsymbol{v}}_2 & \cdots & \overline{\boldsymbol{f}}_K^{\mathrm{H}} \boldsymbol{H}_{K,s} \widehat{\boldsymbol{v}}_K \end{bmatrix}. \tag{22}$$

Note that each entry of $\boldsymbol{H}_{\mathrm{e},s}$ can be obtained from the uplink pilots. The designed digital beamformer under the zero-forcing (ZF) criterion can be expressed as

$$\overline{\boldsymbol{F}}_{\mathrm{BB},s}^{t+1} = \boldsymbol{H}_{\mathrm{e},s} (\boldsymbol{H}_{\mathrm{e},s}^{\mathrm{H}} \boldsymbol{H}_{\mathrm{e},s})^{-1}. \tag{23}$$

Finally, we summarize the proposed beam tracking scheme in **Algorithm 1**

IV. Simulation Results

Now we evaluate the performance of the proposed radar-aided multiuser beam tracking scheme. As shown in Fig. 2, we consider a scenario consisting of two users and one non-cooperative target. The velocity of both the user and the target is set to be 20m/s. Both the transceiver and the receiver at the RSU are equipped with 64 antennas and two RF chains. The number of paths for the two users is set to be 3, where the power ratio between the LoS path and the non-LoS (NLoS) paths is 20 dB. We set $\Delta f = 15$ KHz, $S = 1024$, $P = 375$, $\Delta T = 25$ ms, $\lambda_{\mathrm{c}} = 0.01$ m in OFDM. The radar cross section (RCS) of the target is set to be uniformly distributed between $[10, 100]$ m^2 [11]. The transmit power of the users is set to be 20 dBm. The power of the noise is set to be -109 dBm.

In Fig. 3, we compare the proposed radar-aided multiuser beam tracking scheme with the beam tracking scheme in [6] in terms of the spectral efficiency. The transmit power of the RSU is set to be 40 dBm. To demonstrate the effectiveness of the proposed signal extraction method in Sec. III-A, the performance of independent beam tracking (IBT) of each user is also adopted as a benchmark. It is shown in Fig. 3 that the proposed scheme outperforms the scheme in [6] almost in the whole process of tracking. When the tracking time is less than 5 seconds, the superiority of the proposed scheme mainly comes from the mitigation of the multiuser interference. When the tracking time is greater than 5 seconds, the superiority of the proposed scheme comes from the assistance of the communication to the sensing. In addition, the proposed scheme has similar performance to the IBT, which verifies the effectiveness of the proposed signal extraction method in Sec. III-A.

In Fig. 4, we compare different schemes in terms of the average spectral efficiency of the whole process for various transmit power. It is shown that the proposed scheme outperforms the scheme in [6] for various transmit power. That is because the proposed scheme performs the multiuser interference cancellation and takes the cooperativeness of

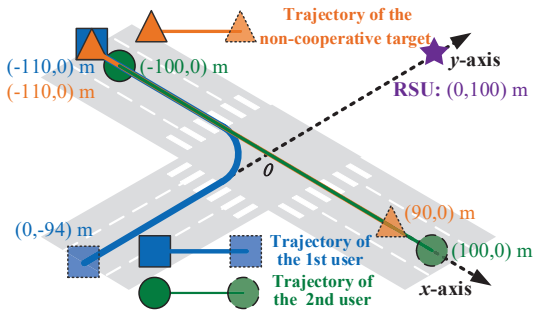

Fig. 2: Illustration of the considered multiuser beam tracking scenario.

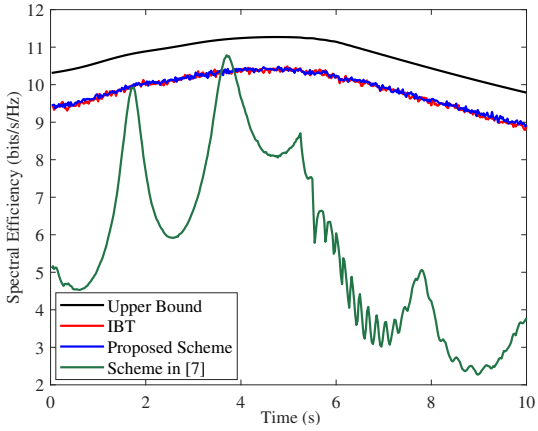

Fig. 3: Comparisons of the spectral efficiency for different schemes.

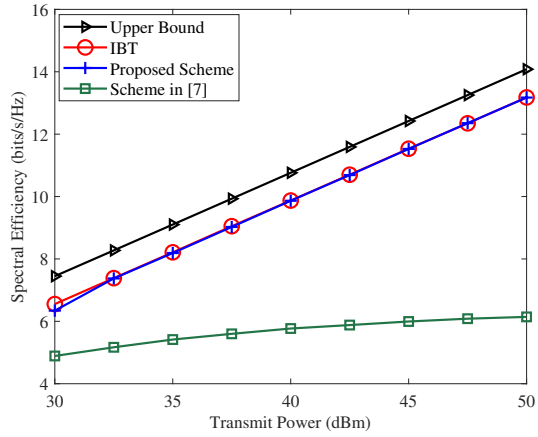

Fig. 4: Comparisons of the average spectral efficiency for different schemes.

the users into consideration, where the former leads to a larger signal-to-interference-and-noise-rate (SINR) and the latter leads to more robust beam alignment. In addition, the proposed scheme can approach the performance of the IBT, which verifies again the effectiveness of the proposed signal extraction method in Sec. III-A.

V. Conclusion

In this paper, radar-aided multiuser beam tracking and target detection has been investigated for ISAC. A multiuser beam tracking scheme based on the collaboration of radar sensing and uplink communication has been proposed. Future work will be continued with efficient beam tracking in ISAC.

VI. Acknowledgment

This work is supported in part by National Natural Science Foundation of China (NSFC) under Grant U22B2007 and 62071116, and by National Key Research and Development Program of China under Grant 2021YFB2900404.

Appendix A

According to (5), we have

$$[\boldsymbol{A}]_{s,p}=\sum_{n=1}^{S}\sum_{t=1}^{P}\frac{[\widetilde{\boldsymbol{x}}_n^{(t)}]_m}{[\widetilde{\boldsymbol{x}}_n^{(t)}]_k}[\boldsymbol{\Lambda}^{(i)}]_{n,t}\mathcal{Z}_P^{-t(p-1)}\mathcal{Z}_S^{n(s-1)}, \quad (24)$$

where $\mathcal{Z}_a^b=e^{2b\pi/a}$. Denote the real part of $[\boldsymbol{A}]_{s,p}$ as $A_{s,p}^{\mathrm{Re}}$ and we have

$$A_{s,p}^{\mathrm{Re}}=\sum_{n=1}^{S}\sum_{t=1}^{P}X_{n,t}^{\mathrm{Re}}\cos\theta_{n,t,s,p}-X_{n,t}^{\mathrm{Im}}\sin\theta_{n,t,s,p}, \quad (25)$$

where

$$\begin{aligned}X_{n,t}^{\mathrm{Re}}&=\mathrm{Re}\{[\widetilde{\boldsymbol{x}}_n^{(t)}]_m[\boldsymbol{\Lambda}^{(i)}]_{n,t}/[\widetilde{\boldsymbol{x}}_n^{(t)}]_k\},\\ X_{n,t}^{\mathrm{Im}}&=\mathrm{Im}\{[\widetilde{\boldsymbol{x}}_n^{(t)}]_m[\boldsymbol{\Lambda}^{(i)}]_{n,t}/[\widetilde{\boldsymbol{x}}_n^{(t)}]_k\},\\ \theta_{n,t,s,p}&=2\pi((s-1)n/S-(p-1)t/P). \end{aligned}\quad (26)$$

Note that $\cos\theta_{n,t,s,p}$ and $\sin\theta_{n,t,s,p}$ in (25) are constants with $|\cos\theta_{n,t,s,p}|\le 1$ and $|\sin\theta_{n,t,s,p}|\le 1$, while $X_{n,t}^{\mathrm{Re}}$ and $X_{n,t}^{\mathrm{Im}}$ are random variables regarding the randomness of $\boldsymbol{x}_n^{(t)}$. We assume $\mathbb{E}\{[\widetilde{\boldsymbol{x}}_n^{(t)}]_m\}=0$, $|[\widetilde{\boldsymbol{x}}_n^{(t)}]_m|\neq 0$, $\max|[\widetilde{\boldsymbol{x}}_n^{(t)}]_m|=A_{\max}$, $\min|[\widetilde{\boldsymbol{x}}_n^{(t)}]_m|=A_{\min}$, $\mathbb{E}\{1/|[\widetilde{\boldsymbol{x}}_n^{(t)}]_m|^2\}=\zeta^2$ and $\mathrm{Var}\{[\widetilde{\boldsymbol{x}}_n^{(t)}]_m\}=\xi^2$. Define $\gamma_{n,t}\triangleq X_{n,t}^{\mathrm{Re}}\cos\theta_{n,t,s,p}-X_{n,t}^{\mathrm{Im}}\sin\theta_{n,t,s,p}$, $\mu_{n,t}\triangleq\mathbb{E}\{\gamma_{n,t}\}$, $\rho_{n,t}^2\triangleq\mathrm{Var}\{\gamma_{n,t}\}$ and $C^2\triangleq\mathrm{Var}\{A_{s,p}^{\mathrm{Re}}\}$. We have

$$\begin{aligned}&\mu_{n,t}=\mathbb{E}\{X_{n,t}^{\mathrm{Re}}\}\cos\theta_{n,t,s,p}+\mathbb{E}\{X_{n,t}^{\mathrm{Re}}\}\sin\theta_{n,t,s,p}=0,\\ &\rho_{n,t}^2\le\mathrm{Var}\{[\widetilde{\boldsymbol{x}}_n^{(t)}]_m[\boldsymbol{\Lambda}^{(i)}]_{n,t}/[\widetilde{\boldsymbol{x}}_n^{(t)}]_k\}\le\xi^2\zeta^2,\\ &C^2=\sum_{n=1}^{S}\sum_{t=1}^{P}\rho_{n,t}^2.\end{aligned}\quad (27)$$

$\forall\epsilon>0$, we have

$$\begin{aligned}&\int_{\left\{x\middle||x|\ge\epsilon C\right\}}(x-\mu_{n,t})^2f_{n,t}(x)dx\\ &\le G_{\max}^2\xi^2\zeta^2P\{|\gamma_{n,t}|\ge\epsilon C\}\overset{(a)}{\le}\frac{G_{\max}^2\xi^2\zeta^2\rho_{n,t}^2}{\epsilon^2C^2},\end{aligned}\quad (28)$$

where $f_{n,t}(x)$ denotes the distribution function of $\gamma_{n,t}$ and (a) holds because of the Chebyshev inequality [15]. Then, we have

$$\frac{1}{C^2}\sum_{n=1}^{S}\sum_{t=1}^{P}\int_{\left\{x\middle||x|\ge\epsilon C\right\}}x^2f_{n,t}(x)dx\le\frac{G_{\max}^2\xi^2\zeta^2}{\epsilon^2C^2}. \quad (29)$$

Note that $\lim_{S,P\to\infty}C^2=\infty$, and $\lim_{S,P\to\infty}\frac{G_{\max}^2\xi^2\zeta^2}{\epsilon^2C^2}=0$. We have

$$\lim_{S,P\to\infty}\frac{1}{C^2}\sum_{n=1}^{S}\sum_{t=1}^{P}\int_{\{x:|x|\ge\epsilon C\}}x^2f_{i,l}(x)dx=0, \quad (30)$$

which indicates that the Lindeberg's condition is satisfied [15]. According to the the Lindeberg-Feller theorem, $A_{s,p}^{\mathrm{Re}}$ converges to $\mathcal{N}(0,C^2)$. Similarly, $A_{s,p}^{\mathrm{Im}}$ converges to $\mathcal{N}\left(0,\mathrm{Var}\left\{A_{s,p}^{\mathrm{Im}}\right\}\right)$. Then, $[\boldsymbol{A}]_{s,p}=A_{s,p}^{\mathrm{Re}}+j\cdot A_{s,p}^{\mathrm{Im}}$ converges to the complex Gaussian distribution.

References

[1] J. A. Zhang, M. L. Rahman, K. Wu *et al.*, "Enabling joint communication and radar sensing in mobile networks—A survey," *IEEE Commun. Surv. Tut.*, vol. 24, no. 1, pp. 306–345, Oct. 2021.

[2] F. Liu, C. Masouros, A. P. Petropulu *et al.*, "Joint radar and communication design: Applications, state-of-the-art, and the road ahead," *IEEE Trans. Commun.*, vol. 68, no. 6, pp. 3834–3862, Feb. 2020.

[3] Y. He, Y. Cai, H. Mao, and G. Yu, "RIS-Assisted communication radar coexistence: Joint beamforming design and analysis," *IEEE J. Sel. Areas Commun.*, vol. 40, no. 7, pp. 2131–2145, Mar. 2022.

[4] C. Qi, W. Ci, J. Zhang, and X. You, "Hybrid beamforming for millimeter wave MIMO integrated sensing and communications," *IEEE Commun. Lett.*, vol. 26, no. 5, pp. 1136–1140, Mar. 2022.

[5] F. Wang and H. Li, "Joint power allocation for radar and communication co-existence," *IEEE Signal Process. Lett*, vol. 26, no. 11, pp. 1608–1612, Sep. 2019.

[6] F. Liu, W. Yuan, C. Masouros, and J. Yuan, "Radar-assisted predictive beamforming for vehicular links: Communication served by sensing," *IEEE Trans. Wireless Commun.*, vol. 19, no. 11, pp. 7704–7719, Aug. 2020.

[7] W. Yuan, F. Liu, C. Masouros, J. Yuan, D. W. K. Ng, and N. González-Prelcic, "Bayesian predictive beamforming for vehicular networks: A low-overhead joint radar-communication approach," *IEEE Trans. Wireless Commun.*, vol. 20, no. 3, pp. 1442–1456, Nov. 2021.

[8] A. M. Jaradat, A. Naeem, M. I. Sağlam, M. Kartal, and H. Arslan, "Radar-aided communication scheduling algorithm for 5G and beyond networks," *IEEE Access*, vol. 10, pp. 96 403–96 413, Sep. 2022.

[9] C. Qi, P. Dong, W. Ma, H. Zhang, Z. Zhang, and G. Y. Li, "Acquisition of channel state information for mmWave massive MIMO: Traditional and machine learning-based approaches," *Sci. China Inf. Sci.*, vol. 64, no. 8, p. 181301, Aug. 2021.

[10] X. Sun, C. Qi, and G. Y. Li, "Beam training and allocation for multiuser millimeter wave massive MIMO systems," *IEEE Trans. Wireless Commun.*, vol. 18, no. 2, pp. 1041–1053, Feb. 2019.

[11] M. A. Richards, *Fundamentals of Radar Signal Processing*, 2nd ed. New York, NY, USA: McGraw-Hill, 2005.

[12] W. Ma, C. Qi, and G. Y. Li, "High-resolution channel estimation for frequency-selective mmWave massive MIMO systems," *IEEE Trans. Wireless Commun.*, vol. 19, no. 5, pp. 3517–3529, Feb. 2020.

[13] Z. Wang, Q. Liu, M. Li, and W. Kellerer, "Energy efficient analog beamformer design for mmWave multicast transmission," *IEEE Trans. Green Commun. Netw.*, vol. 3, no. 2, pp. 552–564, June 2019.

[14] R. Roy and T. Kailath, "ESPRIT-estimation of signal parameters via rotational invariance techniques," *IEEE Trans. Acoust., Speech, Signal, Process.*, vol. 37, no. 7, pp. 984–995, 1989.

[15] R. Durrett, *Probability: Theory and Examples*, 5th ed. New York, NY, USA: Cambridge university press, 2019.